Effects of Density, Morphology, and Photosynthetic Activity in Seaweeds on Nutrient Absorption from Fish Culture Effluent

Boonanan Kaewduang*, Nittiya Numuean, Jantana Praiboon and Anong Chirapart**

ABSTRACT

The use of seaweed for nutrient absorption in aquaculture effluent has gained significant attention. This study investigated the effects of density and surface area-to-volume (SA:V) ratios of three seaweeds: *Caulerpa lentillifera, Ulva rigida,* and *Gracilaria fisheri,* on nutrient uptake in fish culture effluent. Nutrients absorption of NO_2^-, NO_3^-, NH_4^+, and PO_4^{3-} was measured at algal densities of 10, 20, 30, 40, and 50 g·L^{-1} every hour over a 24 h period. Optimal absorption of NO_2^-, NO_3^- and PO_4^{3-} by all three seaweeds occurred at a density of 30 g·L^{-1} within 24 h; with maximum removal efficiencies for *C. lentillifera* reaching 86.03%, 74.08%, and 100%, respectively; for *U. rigida*, 87.33%, 76.51%, and 100%, and for *G. fisheri*, 87.82%, 73.77%, and 100%, respectively. At 40 g·L^{-1}, both *C. lentillifera* and *U. rigida* achieved 100% NH_4^+ removal within 20 h, while *G. fisheri* showed 100% NH_4^+ removal within 18 h at a density of 20 g·L^{-1}. In this study, *U. rigida* exhibited the highest SA:V ratio (12.99±0.06 cm^2:cm^3), surpassing that of *C. lentillifera* (4.48±0.33 cm^2:cm^3) and *G. fisheri* (4.07±0.17 cm^2:cm^3). The SA:V ratio had a positive correlation with total nitrogen reduction, P_{net} and Fv/Fm. Due to its high SA:V ratio and sheet like morphology, *U. rigida* was the most effective at nutrient absorption compared to the siphonous-like *C. lentillifera* and cylindrical, bush-like *G. fisheri*. These results highlight the influence of photosynthetic response on nutrient absorption with varying algal densities and SA:V ratios, identifying an optimum density of 30 g·L^{-1} for green algae and 40 g·L^{-1} for red algae.

Keywords: Aquaculture effluent, Nutrient removal, Photosynthesis, SA:V ratio, Thai seaweed, Thallus form

INTRODUCTION

Aquaculture has become a major source of global seafood, driving by rising demand (FAO, 2020). To meet this demand, many countries have expanded aquaculture production, often using intensive culture systems, characterized by high stocking densities and intensive feeding, which significantly increased organic waste accumulation within farming systems. Effluent from these intensive systems is typically nutrient-rich, containing high levels of nitrogen compounds, such as NH_4^+-N and NO_3^--N, which when released into nearby water bodies, can cause eutrophication of the waters and negatively impact aquatic ecosystems (Liu *et al*., 2016). While various water treatment approaches have been implemented, they have high operating costs (Ruangchuay *et al*., 2024). Among these methods, water treatment using macroalgae stands out as one of the most cost-effective options.

Over the past decades, seaweed has become a feasible and cost-effective alternative for treating aquaculture effluents due to its low cost and high nutrient uptake efficiency (Chopin *et al*., 2001; Neori *et al*., 2004). Several seaweed species have been used as biofilters in aquaculture effluents. For instance, green seaweed genera such as *Ulva* and *Caulerpa* are well known for their high nutrient uptake capacity (Copertino *et al*., 2009; Gao *et al*.,

Department of Fishery Biology, Faculty of Fisheries, Kasetsart University, Chatuchak, Bangkok, Thailand
*Co-corresponding author: boonanan.ka@ku.th
**Corresponding author: ffisanc@ku.ac.th
Received 9 April 2024 / Accepted 4 December 2024

2018; Manori Bambaranda *et al*., 2019a; 2019b; Kang *et al*., 2021). *Ulva clathrata*, for example, has been reported as highly efficient at removing inorganic nutrients from water effluents (Copertino *et al*., 2009), while *Caulerpa sertularioides* and *Ulva lactuca* have been used to treat effluents and promote growth in shrimp culture (Portillo-Clark *et al*., 2013; Brito *et al*., 2014; Elizondo-González *et al*., 2018). *C. lentillifera* has also demonstrated a strong ability to absorb nitrogen and phosphorus (Manori Bambaranda *et al*., 2019a; 2019b; Kunawongdet, 2020). *Ulva pertusa* and *Codium fragile* have been utilized in integrated fish-seaweed culture system as biofilters for effluent from black rockfish (*Sebastes schlegelii*) tanks (Kang *et al*., 2021). Red algae species, including *Gracilaria* and *Gracilariopsis*, have been shown to effectively absorb nitrogen and phosphorus from aquaculture wastewater (Al-Hafedh *et al*., 2012; Du *et al*., 2013; Liu *et al*., 2016; Badraeni *et al*., 2020). However, nutrient absorption efficiencies and growth patterns vary among seaweed species, with each species effectively reducing nitrogen and phosphorus load in the surrounding water. The nutrient removal efficiency of algae depends not only on the species and density of the algae (Kang *et al*., 2011; Liu *et al*., 2016; Ashkenazi *et al*., 2019; Kang *et al*., 2021) but also on their morphology, in terms of the surface area-to-volume ratio (Rosenberg and Ramus, 1984; Rees, 2003).

In Thailand, green and red seaweeds have been utilized to treat wastewater in aquaculture ponds (Lewmanomont and Chirapart, 2022; Ruangchuay *et al*., 2024). Various Thai seaweed species such as *Caulerpa lentillifera, Ulva rigida, Gracilaria fisheri,* and *G. tenuistipitata* have shown effectiveness in treating aquaculture effluents (Thongcanarak and Predalumpaburt, 2008; Chaitanawisuti *et al*., 2011; Kunawongdet, 2020; Suphawinyoo *et al*., 2020; Hajisamae *et al*., 2022). Nonetheless, there are differences in treatment efficacy across these species. Most studies have focused on the effects of algae density and species on nutrient absorption, while research on morphological changes and physiological responses during nutrient uptake is limited.

This study aimed to assess the nutrient absorption capabilities of the green seaweeds *C. lentillifera* and *U. rigida* and the red seaweed *G. fisheri*, selected for their distinct morphological characteristics. We hypothesized that differences in algal density and thallus structure would impact nutrient removal from fish effluent. Additionally, the photosynthetic responses of these algae at different densities were examined. These findings contribute to a deeper understanding of algal nutrient absorption and help identifying suitable species for aquaculture effluent treatment.

MATERIALS AND METHODS

Fish collection and acclimatization

Sailfin mollies (*Poecilia latipinna*) were purchased from an ornamental fish dealer in Bangkok and transported to the Algal Bioresources Research Center, Kasetsart University for acclimation. Acclimation procedures followed the methods outlined by Manori Bambaranda *et al*. (2019a). The fish were reared in three glass fiber tanks, each measuring 1×0.6×0.5 m and filled with 150 L of dechlorinated freshwater (treated with 30 $mg \cdot L^{-1}$ chlorine). Aeration was provided in each tank using a diaphragm blower with an aeration rate of 50% using an air stone equipped with an air controller. Forty *P. latipinna* fish (3–5 cm in size) were stored in each tank at a male:female ratio of 1:1. Ten fish from each tank were randomly selected and weighed, and the feeding rate was calculated, with the amount of feed given as 4% of the fish weight. The fish were fed twice daily at 9:00 am and 4:00 pm, and uneaten feed was removed by siphoning after 5–7 min. Bottom siphoning was performed once daily, followed by refilling the tanks with treated water to maintain a 150 L volume. Following one week of acclimation, the water salinity in the tanks was gradually increased by 5‰ every three days, from 0‰ to 30‰, using concentrated, chlorine-treated seawater (30 $mg \cdot L^{-1}$). Once the tanks reached 30‰, salinity and water volume were maintained at these levels. Salinity was monitored twice daily with a refractometer (S/Mill-E, ATAGO, Japan). Before each feeding and siphoning, a 1-litter water sample was collected from each tank to measure nutrient content. The water samples were filtered using GF/C Whatman filter paper (0.45 µm).

The dissolved inorganic nitrogen (nitrite, nitrate, ammonia) and orthophosphate levels were measured (n = 3) following to the standard methods for water and wastewater analysis, including the cadmium reduction method, naphthyl ethylenediamine method, phenate method, and ascorbic acid method. A UV–visible spectrophotometer (Shimadzu UV-1061) was used at wavelengths of 543, 543, 640, and 880 nm, respectively (APHA, 2005). After 7 days of acclimation, fish effluent samples were analyzed to determine whether dissolved nutrient concentrations exceeded Thailand's Coastal Aquaculture Effluent Standards. These standards specify that ammonia should not exceed 1.1 $mg \cdot L^{-1}$, total nitrogen should not exceed 4.0 $mg \cdot L^{-1}$, and phosphorus should not exceed 0.5 $mg \cdot L^{-1}$ (Notification of the Ministry of Natural Resources and Environment, 2004).

Seaweed preparation

The green seaweed species, *Caulerpa lentillifera* and *Ulva rigida* were collected from seaweed farms in Pattani and Satun Provinces, respectively. The red seaweed *Gracilaria fisheri* was sourced from the coast of Samaesan (12°39′47″N 100°54′20″E) in Chonburi Province. Samples were cleaned of visible contaminants and acclimated in seawater at 30‰ salinity within an indoor greenhouse for 21 days.

Seaweed density

After 21 days of acclimation, healthy samples of each species, selected for similar weight and length, were used. Whole thallus samples were chosen based on the natural forms of each species. Five stocking densities (10, 20, 30, 40, and 50 $g \cdot L^{-1}$) were examined in triplicate using a completely randomized design (CRD).

The fish effluent (from clause 1) was filtered through 0.45 µm GF/C Whatman filter paper. A nonreactive plastic bottle (6×6×15 cm) containing 300 mL of filtered fish effluent (n = 24 per replicate) was used for the experiment. Different densities were tested in triplicate, with hourly nutrient absorption monitored in separate experimental units. Algal samples were removed every hour for up to 24 h, and absorption levels of NO_2^--N, NO_3^--N, NH_4^+-N, and PO_4^{-3}-P were measured according to APHA (2005). The experiment was conducted under controlled conditions at 30‰ salinity, 25±2 °C temperature, and a light intensity of 105 µmol photon$\cdot m^{-2} \cdot s^{-1}$ on a 12:12 h light:dark cycle. Nutrient absorption efficiency was calculated as follows:

$$\text{Absorption efficiency (\%)} = (N_0\text{-}N_t)/\ N_0 \times 100$$

where N_0 is the initial nutrient concentration, and N_t is the nutrient concentration at time *t* (hours).

Determination of seaweed surface area-to-volume ratio

The surface area-to-volume (SA:V) ratio was measured according to the morphology of each seaweed species. For *U. rigida*, the width and length of sheet-like thalli were randomly measured using Vernier calipers, and thickness was measured from transverse sections (n = 24) under a light microscope. The surface area and volume of each alga were calculated using the following geometric equations (Vogel, 1988):

$$\text{Surface area } (cm^2) = \text{width} \times \text{length};$$

$$\text{Volume } (cm^3) = \text{width} \times \text{length} \times \text{height}.$$

For *C. lentillifera* and *G. fisheri*, lengths were measured with Vernier calipers, and thickness was measured from transverse sections under a light microscope. The surface area and volume of the samples were calculated using the following geometric equations (Vogel, 1988):

$$\text{Surface area } (cm^2) = 2\pi r \times \text{thallus length};$$

$$\text{Volume } (cm^3) = \pi r^2 \times \text{thallus length}.$$

Photosynthesis determination

The algal samples at each density used for nutrient absorption (in clause 3) were measured for photosynthesis. Changes in the photosynthetic efficiency (Fv/Fm) of photosystem II (PSII) were measured using a Junior-PAM (Pluse-Amplitude-Modulation) chlorophyll fluorometer after the

whole thallus samples were incubated in the dark for 30 min. Photosynthetic efficiency was calculated using the following formula:

$$Fv/Fm = (Fm - Fo)/Fm,$$

where Fm is the maximum fluorescence and Fo is the minimal fluorescence (Maxwell and Johnson, 2000).

The relative electron transport rate (rETR) of each algal sample (1 g wet weight per sample, n = 20) was determined under laboratory conditions. Rapid light curves (RLCs) were generated by applying the standard algorithm of a pulse amplitude modulated (PAM) fluorometer (Junior PAM, Walz/Germany) in an incremental sequence of actinic illumination periods, with light intensity (photosynthetically active radiation, PAR) increasing in nine steps from 0 to 625 µmol photons·m^{-2}·s^{-1}. The rETR was calculated using the equation:

$$rETR = 0.5 \times Y \times PAR \times AF$$

where Y represents the effective quantum yield of photosystem II (PSII), the factor 0.5 assumes that half of the photons are absorbed by PSII, and AF is the fraction of incident light assumed to be absorbed by the sample (≈ 0.84) (Schreiber *et al*., 1995).

Photosynthetic rates were measured at each density under 25±2 °C and 105 µmol photon·m^{-2}·s^{-1} light intensity on a 12:12 h light:dark cycle. The photosynthetic rates were determined by the light/dark bottle technique, with net photosynthetic rate (P_{net}) and dark respiration measured as dissolved oxygen (mg·L^{-1}) every 5 min for 30 min using a DO meter (YSI 5000).

Statistical analysis

Results are presented as the mean±standard deviation (SD). Statistical analyses were performed using analysis of variance (ANOVA) followed by Tukey's HSD tests at 95% confidence level. Relationships between variables were assessed using Pearson's correlation coefficient, also at a 95% confidence level.

RESULTS

Effects of density on nutrient uptake

Changes in the concentrations of nitrite (NO_2^-), nitrate (NO_3^-), ammonia (NH_4^+) and orthophosphate (PO_4^{3-}) over time at different algal densities (10, 20, 30, 40 and 50 g·L^{-1}) are shown in Figures 1–3. Variation in algal density influenced the reduction in nutrient concentrations in the fish effluent. *Caulerpa lentillifera* showed the greatest reductions in NO_2^--N and NO_3^--N at a density of 30 g·L^{-1}, followed by densities of 40, 20, 50, and 10 g·L^{-1}, respectively (Figure 1). At these densities, the maximum removal efficiency of NO_2^--N was 86.03%, 70.73%, 67.99%, 61.63% and 51.03%, respectively; the removal efficiencies of NO_3^--N were 74.08%, 63.44%, 56.89%, 55.99%, and 49.00%, respectively. However, NO_3^- reduction at 20 and 50 g·L^{-1} was not significantly different ($p \geq 0.05$). All densities of *C. lentillifera* achieved 100% NH_4^+ absorption. At a density of 40 g·L^{-1}, ammonia was completely absorbed within 20 h, while at densities of 30, 10, 50, and 20 g·L^{-1}, it required 21, 21, 22, and 23 h, respectively, for complete NH_4^+-N uptake. This species also effectively removed orthophosphate from the fish effluent. At 10, 20, and 30 g·L^{-1}, *C. lentillifera* reduced PO_4^{3-}-P by 100% within 24, 19, and 18 h, respectively. However, absorption efficiency of PO_4^{3-}-P decreased when the densities increased to 40 g·L^{-1} (82.34%) and 50 g·L^{-1} (67.42%).

Similar to *C. lentillifera, U. rigida* exhibited the greatest absorption of NO_2^--N and NO_3^--N at a density of 30 g·L^{-1}, achieving efficiencies of 87.33% and 76.51%, respectively. Absorption efficiencies decreased at densities of 40, 50, 20, and 10 g·L^{-1}, with NO_2^--N absorption efficiencies of approximately 73.47%, 70.98%, 65.22% and 55.60%, and NO_3^--N absorption rates of 76.51%, 66.86%, 63.44%, 60.06% and 53.77%, respectively. At all densities, *U. rigida* achieved complete NH_4^+- absorption (100%) within 24 h, with the fastest absorption at a density of 40 g·L^{-1} within 19 h. At densities of 30, 10, 50, and 20 g·L^{-1}, NH_4^+ was fully absorbed within 21, 21, 22 and 23 h, respectively. The algae also achieved 100% PO_4^{3-} absorption within 23, 19, and 18 h at densities of 10, 20, and 30 g·L^{-1}, respectively. However, PO_4^{3-} absorption efficiencies decreased

to 84.00% and 70.46% at densities of 40 and 50 g·L^{-1}, respectively (Figure 2).

Similarly, varying densities of *G. fisheri* influenced nutrient uptake within a 24 h period (Figure 3). *G. fisheri* showed the greatest absorption of NO_2^--N and NO_3^--N at a density of 30 g·L^{-1}. The highest absorption efficiencies of nitrite were 87.82%, 74.47%, 72.06%, 66.48% and 57.14% at 30, 40, 50, 20 and 10 g·L^{-1}, respectively; the corresponding nitrate concentrations were 73.77%, 62.99%, 56.28%, 55.32%, and 48.28% at 30, 40, 20, 50, and 10 g·L^{-1}, respectively. At a density of 20 g·L^{-1}, *G. fisheri* achieved complete absorption of NH_4^+ (100%) within 18 h. In contrast, at densities of 30, 10, 50, and 40 g·L^{-1}, the algae achieved full NH_4^+ uptake within 21, 21, 22 and 23 h, respectively. PO_4^{3-} absorption was also highly efficient, with *G. fisheri* achieving 100% reduction at densities of 20 and 30 g·L^{-1} within 20 and 19 h, respectively. PO_4^{3-} absorption apparently decreased to 99.08% at 10 g·L^{-1} and further dropped at higher densities, reaching 82.13% at 40 g·L^{-1} and 67.03% at 50 g·L^{-1}.

Our study revealed a relationship between seaweed density and nutrient absorption from fish effluent. The density of all three algae species showed a positive correlation with the total nitrogen uptake rate ($p<0.05$). At densities of 10–30 g·L^{-1}, *U. rigida* was positively correlated with PO_4^{3-} reduction ($r = 0.999$, $p = 0.031$), while the correlation of *C. lentillifera* and *G. fisheri* were not significant ($p\geq0.05$). At higher densities of 40 and 50 g·L^{-1}, PO_4^{3-} absorption in *C. lentillifera* and *G. fisheri* was negatively correlated ($r = -0.999$, $p = 0.034$).

Photosynthetic responses to algae density

This study showed that algae density affected the photosynthetic activity of *C. lentillifera, U. rigida,* and *G. fisheri*. The electron transport rates (rETRs) of photosystem II (PS II) in all three species varied with light intensity (photosynthetically active radiation, PAR), with ETR increasing as light intensity rose up to 625 µmol photons·m^{-2}·s^{-1}. In *C. lentillifera*, ETRs at all densities followed a similar trend, rising with light intensities between

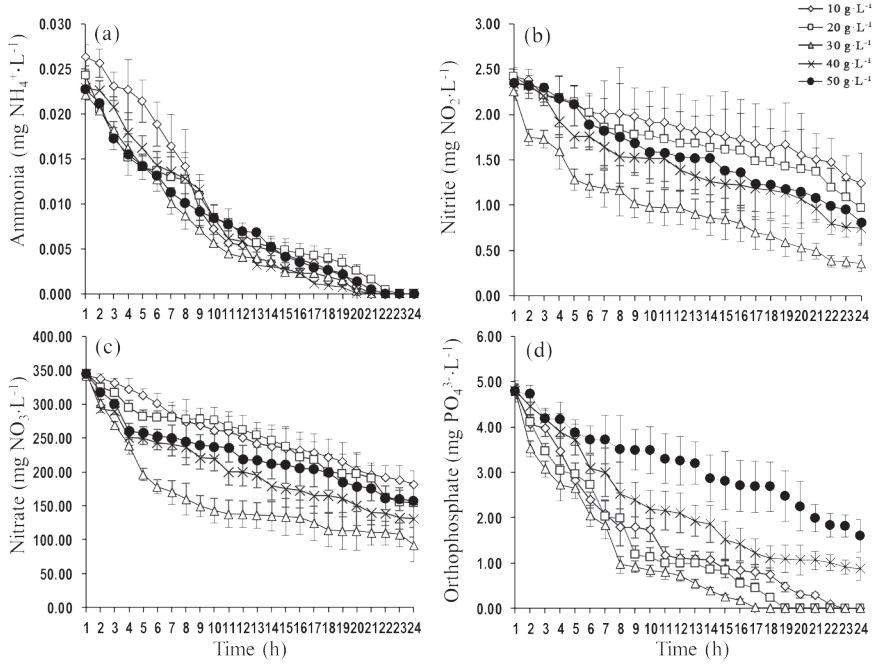

Figure 1. Changes over time in the concentrations of: (a) ammonia (NH_4^+), (b) nitrite (NO_2^-), (c) nitrate (NO_3^-), and (d) orthophosphate (PO_4^{3-}) in fish effluent treated with *Caulerpa lentillifera* at five algal density levels (10, 20, 30, 40, and 50 g·L^{-1}) under conditions of 30‰ salinity, and 25 °C. Vertical bars represent standard deviations (n = 3).

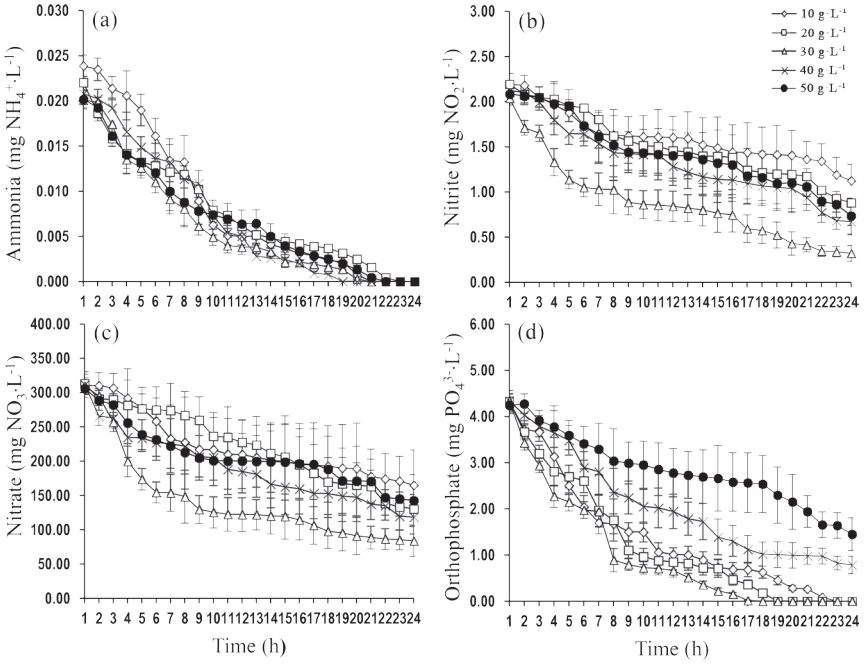

Figure 2. Changes over time in the concentrations of: (a) ammonia (NH_4^+), (b) nitrite (NO_2^-), (c) nitrate (NO_3^-), and (d) orthophosphate (PO_4^{3-}) with *Ulva rigida* at five algal density level (10, 20, 30, 40, and 50 g·L^{-1}) under conditions of 30‰ salinity, and 25 °C. Vertical bars represent standard deviations (n = 3).

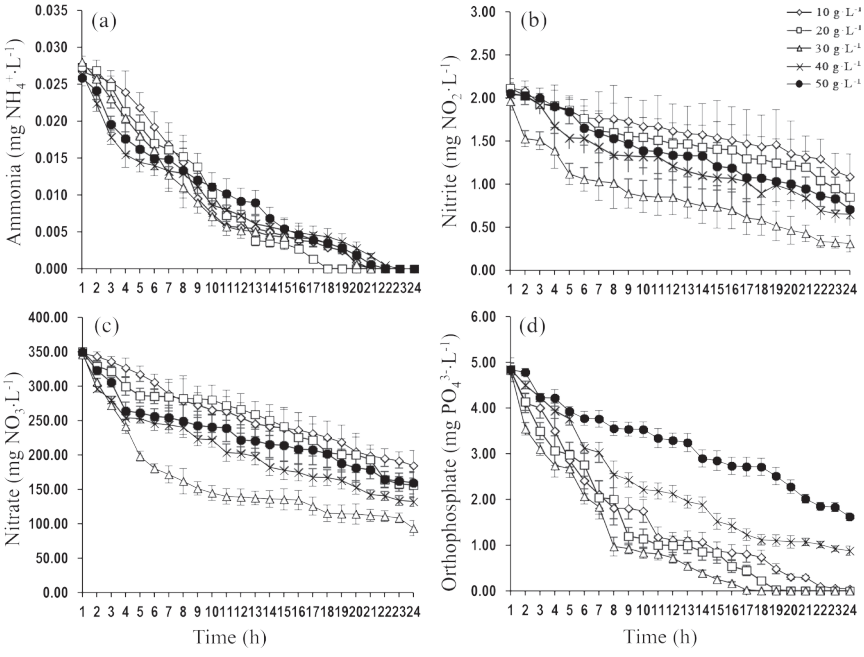

Figure 3. Changes over time in concentration of ammonia (NH_4^+), nitrite (NO_2^-), nitrate (NO_3^-), and orthophosphate (PO_4^{3-}) with *Gracilaria fisheri* at five algal density level (10, 20, 30, 40, and 50 g·L^{-1}), 30‰ salinity, and 25 °C temperature. The vertical bars indicate standard deviations (n = 3).

0 and 425 µmol photons·m^{-2}·s^{-1}. However, ETRs differed across species at a light intensity of 625 µmol photons·m^{-2}·s^{-1}, with the highest ETR of 22.60± 0.87 µmol e·m^{-2}·s^{-1} observed at 30 g·L^{-1}. Similar ETR values were recorded at 40, 20, 10, and 50 g·L^{-1}, measuring 21.50±0.17, 21.07±0.78, 20.87± 0.58, and 20.27±0.12 µmol e·m^{-2}·s^{-1}, respectively (Figure 4a).

In *U. rigida*, ETR increased with light intensity across all densities from 0 to 625 µmol photons·m^{-2}·s^{-1}. At a density of 30 g·L^{-1}, the ETR rose sharply with increasing light intensity from 25 to 625 µmol photons·m^{-2}·s^{-1}, reaching a peak of 27.57±0.32 µmol e·m^{-2}·s^{-1}. Other densities, 20, 10, 40, and 50 g·L^{-1}, produced maximum ETR values of 21.30±0.36, 20.57±0.64, 20.13±0.06, and 18.37± 0.47 µmol e·m^{-2}·s^{-1}, respectively (Figure 4b).

For *G. fisheri*, density had a similar effect on ETR as in other species, with increases in ETR at light intensities up to 625 µmol photons·m^{-2}·s^{-1}. However, there were no significant differences in ETR ($p \geq 0.05$) between densities, with ETR values of 21.40±0.17, 21.07±0.78, 20.70±0.52, 20.60±0.62 and 20.17±0.06 µmol e·m^{-2}·s^{-1} at densities of 40, 20, 10, 30, and 50 g·L^{-1}, respectively (Figure 4c).

This study revealed similar responses in gross (GPP) and net photosynthetic rate (P_{net}) among the three seaweed species in response to density (Figure 5). The GPP and P_{net} of both *C. lentillifera* and *U. rigida* were highest at 30 g·L^{-1}, with GPP values of 3.42±0.01 and 7.07±0.16 µgO_2·g^{-1}_{ww}·min^{-1} and P_{net} values of 2.78±0.01 and 6.37±0.15 µgO_2·g^{-1}_{ww}·min^{-1}), respectively. For *G. fisheri* peak GPP (2.92±0.06 µgO_2·g^{-1}_{ww}·min^{-1}) and P_{net} values (2.28±0.07 µgO_2·g^{-1}_{ww}·min^{-1}) were reached at a density of 40 g·L^{-1}. Across all densities, *U. rigida* had significantly greater GPP and P_{net} values than *C. lentillifera* and *G. fisheri* ($p<0.05$), with *C. lentillifera* also outperforming *G. fisheri* at densities of 20 and 30 g·L^{-1}.

The relationship between density and photosynthesis aligned with that between nutrient absorption and photosynthesis. *C. lentillifera* and *U. rigida* densities of 10–30 g·L^{-1} positively correlated with P_{net} ($r = 0.999$, $p = 0.031$ and $r = 0.999$, $p = 0.023$, respectively). However, at higher densities (30–50 g·L^{-1}), both species exhibited a negative correlation with P_{net} ($r = -0.997$, $p = 0.047$ for *C. lentillifera* and $r = -1.000$, $p = 0.015$ for *U. rigida*). For *G. fisheri*, densities of 10–40 g·L^{-1} positively correlated with P_{net} ($r = 0.975$, $p = 0.025$), while a negative correlation ($r = -1.000$, $p = 0.002$) was observed at 40–50 g·L^{-1}.

Our study also demonstrated that algal density influenced the photosynthetic efficiency (Fv/Fm) of the three seaweed species (Figure 6). The average Fv/Fm values for *U. rigida, C. lentillifera,* and *G. fisheri* were 0.662–0.699, 0.557–0.637, and 0.552–0.611, respectively. At a density of 30 g·L^{-1}, the Fv/Fm values of *U. rigida* and *C. lentillifera* were 0.699±0.015 and 0.637±0.005, respectively, while *G. fisheri* reached an Fv/Fm value of 0.611± 0.002 at 40 g·L^{-1}. The Fv/Fm of *U. rigida* was significantly higher than that of *C. lentillifera* and *G. fisheri* at the same algae density ($p<0.05$).

Relationships of the SA:V ratio with nutrient absorption and photosynthesis in the seaweeds

In this study, the SA:V ratio of *U. rigida* was significantly higher (12.99±0.06 cm^2:cm^3) than those of *C. lentillifera* (4.48±0.33 cm^2:cm^3) and *G. fisheri* (4.07±0.17 cm^2:cm^3). The SA:V ratios were significantly different among the three algae ($p<0.05$). We analyzed the relationships between the SA:V ratio of each seaweed and the uptake of total nitrogen and photosynthesis at a density of 30 g·L^{-1} under 12 h of light exposure. The SA:V ratio of the three algal species were positively correlated with the reduction of total nitrogen in the fish effluent ($r = 0.997$, $p = 0.047$). The SA:V ratio also showed a near significant positive correlation with P_{net} ($r = 0.997$, $p = 0.050$), and a significant correlation with Fv/Fm ($r = 0.999$, $p = 0.024$) in the algae. Additionally, the total nitrogen uptake rate was significantly positively correlated with P_{net} in the algae ($r = 1.000$, $p = 0.002$).

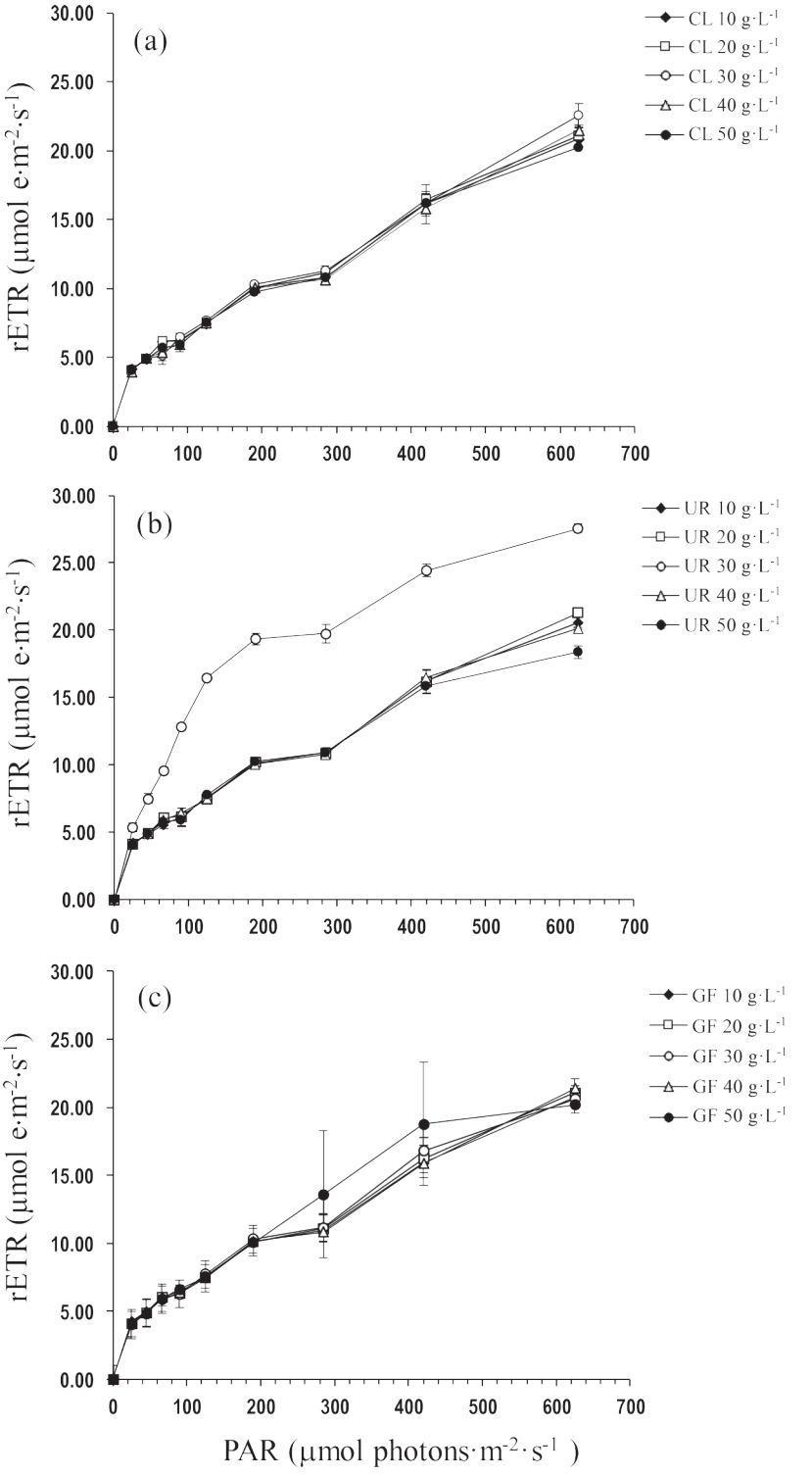

Figure 4. Responses to irradiance levels between 0–625 µmol photons·m^{-2}·s^{-1} on the relative electron transport rate (rETR) of Chl *a* fluorescence of *Caulerpa lentillifera* (a), *Ulva rigida* (b), and *Gracilaria fisheri* (c) at densities of 10, 20, 30, 40, and 50 g·L^{-1}. Vertical bars represent standard deviations (n = 3).

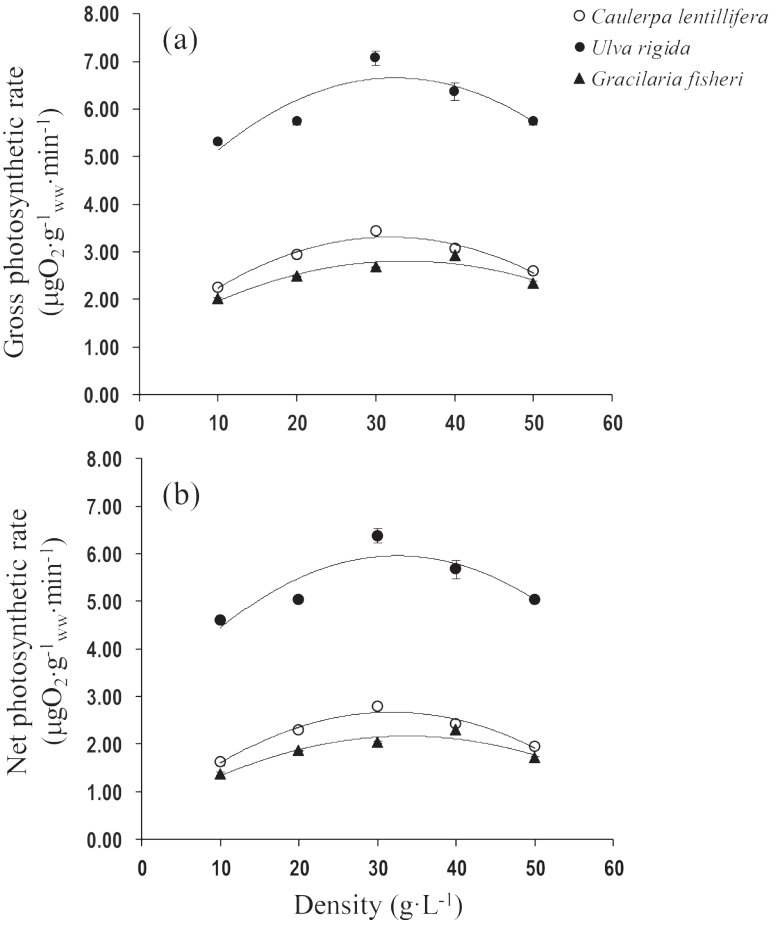

Figure 5. Responses of gross and net photosynthesis to varying densities of *Caulerpa lentillifera, Ulva rigida,* and *Gracialria fisheri* at levels of 10, 20, 30, 40, and 50 g·L^{-1}. Vertical bars represent standard deviations (n = 3).

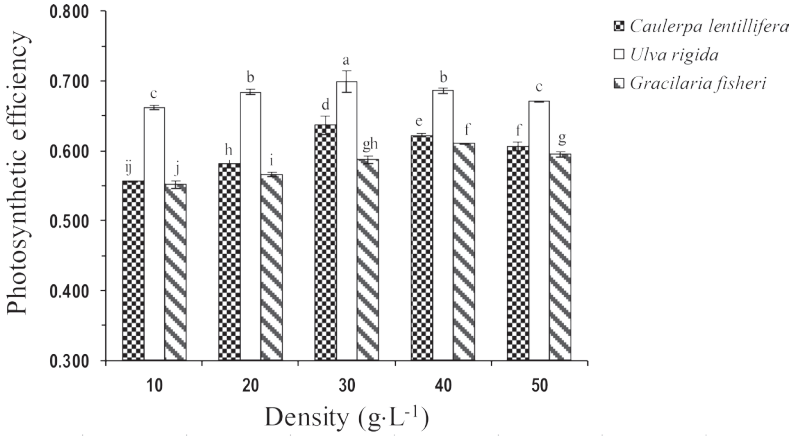

Figure 6. Responses of photosynthetic efficiency (Fv/Fm) to varying densities of *Caulerpa lentillifera, Ulva rigida* and *Gracilaria* fisheri at levels of 10, 20, 30, 40, and 50 g·L^{-1}. Vertical bars represent standard deviations (n = 3), and different letters above bars represent significant differences ($p<0.05$).

DISCUSSION

Seaweeds, are known for their ability to reduce nutrients in aquaculture effluent, whereby the efficiency varies with species and strain of algae (Liu *et al*., 2016; Ashkenazi *et al*., 2019; Khan *et al*., 2021). Nutrient uptake efficiency is influenced by major factors such as density of the algae (Al-Hafedh *et al*., 2012; 2014; Li *et al*., 2020) and the morphology of the seaweed (Gacia *et al*., 1996; Stewart and Carpenter, 2003). An increase in algal density reduces the flow velocity of seawater and thickens the diffusion boundary layer around the surface of the algal thalli. This decrease in flow velocity reduces the absorption of light, nutrients, and dissolved inorganic carbon (Hurd, 2000), as well as photosynthetic capacity (Gaylord *et al*., 2007). In the present study, the density of algae was related to nutrient absorption from fish effluent. A positive correlation was observed at densities of 10–30 $g \cdot L^{-1}$ for nitrogen and 10–40 $g \cdot L^{-1}$ for phosphorus nutrients, with the most effective nutrient removal occurring at 30 $g \cdot L^{-1}$. Similarly, Manori Bambaranda *et al*. (2019a) reported that *Caulerpa* seaweed as effectively reduce NO_2^--N, NO_3^--N, NH_4^+-N, and PO_4^{-3}-P in the effluent of sailfin mollies, with the highest removal efficiency at densities of 31.6, 33.3, 50.0, and 20.0 $g \cdot L^{-1}$, respectively. However, *C. lentillifera* was reported to have the greatest reduction of nutrients from the effluent of cultured anemone fish at a lower density of 2 $g \cdot L^{-1}$ (Kunawongdet, 2020). In this study, the removal efficiency of PO_4^{3-}-P did not differ significantly between the two green species, *C. lentillifera* and *U. rigida*. Additionally, nitrogen nutrient uptake efficiency, but not ammonia uptake, was similar between the green algae and the red algae.

A limitation in nutrient uptake by these seaweeds at both lower and higher seaweed densities may be due to limited algal biomass at low densities and self-shading at high densities (Manori Bambaranda *et al*., 2019a; Li *et al*., 2020). Changes in algal density result in complex photophysiological responses to variations in pH and temperature (Li *et al*., 2020). In addition, an increase in algal density could reduce the amount of inorganic carbon received per unit biomass, which limits photosynthesis and reduces photosynthetic O_2 evolution (Jiang *et al*., 2017; Li *et al*., 2020). Increased biomass density significantly reduced the photosynthetic capacity of the algae. This can be explained by the shading effect caused by the density, where thalli block light from each other, reducing the light flux on individual surfaces (Hurd, 2000; Stewart and Carpenter, 2003). As a result, light-utilization efficiency is reduced, which consequently lowers the photosynthetic rate and promotes saturation light levels (Copertino *et al*., 2009; Richards *et al*., 2011; Jiang *et al*., 2017).

The nutrient absorption capacity depends not only on the density of the algae but also on morphological changes. Seaweeds with a high surface-to-volume (SA:V) ratio have a higher nutrient uptake rate due to the increased membrane surface area available for uptake (Taylor *et al*., 1998). In this study, the different morphological characteristics among the three seaweed species revealed that *U. rigida* has the simplest cell structure. The absorption of nutrients by the seaweeds was correlated with the morphology (SA:V ratio) of the algae. A positive correlation between nutrient uptake and the SA:V ratio of the three seaweeds was consistent with the findings of a previous study (Rosenberg and Ramus, 1984), which reported a positive correlation between uptake rates and the SA:V ratio of the thallus (*Ulva curvata* > *Fucus evanescens* ≈ *Gracilaria tikvahiae* > *Codium decorticatum*). Rosenberg and Ramus (1984) reported that lower rates of nutrient uptake are associated with lower SA:V ratios. In this study, the high SA:V ratio of the sheet-like *U. rigida* increased the efficacy of nutrient uptake compared to the other two algae, which had lower SA:V ratios. Moreover, the high efficiency of *U. rigida* may be due to the greater membrane surface area available for nutrient uptake (Taylor *et al*., 1998). A high SA:V ratio allows this seaweed to rapidly assimilate nutrients (Rosenberg and Ramus, 1984; Rees, 2003; Neori *et al*., 2004). Notably, ammonia can be passively absorbed by *U. rigida*, with the conversion of NH_4^+ to NH_3 at the thalli surface. A linear relationship between the rate of NH_4^+ uptake (per g DW) and NH_4^+ concentration has been reported for algae such as *Xiphophora chondrophylla* (with a low SA:V ratio) and *Ulva* sp. (with a high SA:V ratio); suggesting that ammonia uptake occurs via passive diffusion of NH_4^+ (Taylor *et al*., 1998).

Additionally, the SA:V ratio was positively correlated with increased P_{net} and photosynthetic efficiency in these seaweeds. In other words, an increased SA:V ratio results in higher photosynthesis efficiency and P_{net}. Differences in the thalli forms resulted in higher P_{net} and R_d in the sheet-like cells of *U. rigida* (high SA:V ratio), and lower P_{net} and R_d in the siphonous alga *C. lentillifera* and cylindrical, bush-like alga *G. fisheri* (low SA:V ratio). This study confirmed the role of morphology in these three seaweeds, showing that it affects the area exposed to light and the sites of ion exchange. Thus, differences in the SA:V ratio of algae could impact the rate of photosynthesis (Mauseth, 2000). Johansson and Snoeijs (2002) stated that photosynthetic capacity is dependent on the morphology of the algae, with thinner and more filamentous species reflecting higher rate of O_2 production, while thicker and coarser species have lower rates. A previous study reported a decrease in the productivity of *Caulerpa* with increasing morphological complexity (Gacia *et al*., 1996). Furthermore, a recent study reported that the thinner form of filamentous green alga (*Oedogonium*) had a greater photosynthetic rate than its thicker counterpart (Rattanasaensri *et al*., 2020).

CONCLUSIONS

In this study, the seaweeds *Cauelerpa lentillifera, Ulva rigida,* and *Gracilaria fisheri* were highly effective at removing inorganic nitrogen (NH_4^+-N, NO_2^--N, and NO_3^--N) and PO_4^{3-}-P from the effluent of sailfin mollies. Changes in the density of these seaweeds affected nutrient reduction efficiency. These three seaweeds showed the highest efficiencies in removing NO_2^--N and NO_3^--N at a density of 30 $g \cdot L^{-1}$. *C. lentillifera* and *U. rigida* showed the highest NH_4^+-N removal efficiency (100%) at a density of 40 $g \cdot L^{-1}$, while *G. fisheri* reached this efficiency at 20 $g \cdot L^{-1}$. The removal efficiency of PO_4^{3-}-P did not differ between the two green seaweed species. Additionally, the efficiency of reducing inorganic nitrogen was not significantly different between the green algae and the red algae, except for ammonia. Among the three seaweeds, the sheet-like *U. rigida* was the most effective at reducing inorganic compounds (both nitrogen and phosphorus), as reflected by its relatively high SA:V ratio. On the other hand, the photosynthetic responses to algae density tended to be similar among the three seaweed species. However, *U. rigida* exhibited the greatest nutrient removal efficiency and photosynthetic performance at the same algae density. Our study suggests that an algae density of 30 $g \cdot L^{-1}$ is optimal for the uptake of inorganic nitrogen in effluent from an aquaculture system. However, these results are based on short-term laboratory measurements. Further research is needed to investigate the factors affecting the nutrient absorption performance of these seaweeds, such as light, temperature, salinity, and water movement.

ACKNOWLEDGEMENTS

This work was supported by the Algal Bioresources Research Center, Department of Fishery Biology, Kasetsart University. The authors are grateful to anonymous reviewers whose remarks helped to improve this paper.

LITERATURE CITED

Al-Hafedh, Y.S., A. Alam, A.H. Buschmann and K.M. Fitzsimmons. 2012. Experiments on an integrated aquaculture system (seaweeds and marine fish) on the Red Sea coast of Saudi Arabia: efficiency comparison of two local seaweed species for nutrient biofiltration and production. **Reviews in Aquaculture** 4(1): 21–31. DOI: 10.1111/j.1753-5131.2012.01057.x.

Al-Hafedh, Y.S., A. Alam and A.H. Buschmann. 2014. Bioremediation potential, growth and biomass yield of the green seaweed, *Ulva lactuca* in an integrated marine aquaculture system at the Red Sea coast of Saudi Arabia at different stocking densities and effluent flow rates. **Reviews in Aquaculture** 6: 1–11. DOI: 10.1111/raq.12060.

American Public Health Association (APHA). 2005. **Standard Methods for the Examination of Water and Wastewater,** 21st ed. American Public Health Association/ American Water Works Association/Water Environment Federation, Washington, D.C., USA. 1288 pp.

Ashkenazi, D.Y., A. Israel and A. Abelson. 2019. A novel two-stage seaweed integrated multi-trophic aquaculture. **Reviews in Aquaculture** 11: 246–262. DOI: 10.1111/raq.12238.

Badraeni, B., H. Azis, J. Tresnati and A. Tuwo. 2020. Seaweed *Gracilaria changii* as a bioremediator agent for ammonia, nitrite and nitrate in controlled tanks of whiteleg shrimp *Litopenaeus vannamei*. **IOP Conference Series.: Earth and Environmental Science** 564: 012059. DOI: 10.1088/1755-1315/564/1/012059.

Brito, L.O., R. Arantes, C. Magnotti, R. Derner, F. Pchara, A. Olivera and L. Vinatea. 2014. Water quality and growth of Pacific white shrimp *Litopenaeus vannamei* (Boone) in co-culture with green seaweed *Ulva lactuca* (Linaeus) in intensive system. **Aquaculture International** 22: 497–508. DOI: 10.1007/s10499-013-9659-0.

Chaitanawisuti, N., W. Santhaweesuk and S. Kritsanapuntu. 2011. Performance of the seaweeds *Gracilaria salicornia* and *Caulerpa lentillifera* as biofilters in a hatchery scale recirculating aquaculture system for juvenile spotted babylons (*Babylonia areolata*). **Aquaculture International** 19: 1139–1150. DOI: 10.1007/s10499-011-9429-9.

Chopin, T., A.H. Buschmann, C. Halling, M. Troell, N. Kautsky, A. Neori and C. Neefus. 2001. Integrating seaweeds into marine aquaculture systems: a key toward sustainability. **Journal of Phycology** 37: 975–986. DOI: 10.1046/j.1529-8817.2001.01137.x.

Copertino, M.S., T. Tormena and U. Seeliger. 2009. Biofiltering efficiency, uptake and assimilation rates of *Ulva clathrata* (Roth) J. Agardh (Chlorophyceae) cultivated in shrimp aquaculture waste water. **Journal of Applied Phycology** 21: 31–45. DOI: 10.1007/s10811-008-9357-x.

Du, R., L. Liu, A. Wang and Y. Wang. 2013. Effects of temperature, algae biomass and ambient nutrient on the absorption of dissolved nitrogen and phosphate by Rhodophyte *Gracilaria asiatica*. **Chinese Journal of Oceanology and Limnology** 31: 353–365. DOI: 10.1007/s00343-013-2114-2.

Elizondo-González, R., E. Quiroz-Guzmán, C. Escobedo-Fregoso, P. Magallón-Servín and A. Peña-Rodríguez. 2018. Use of seaweed *Ulva lactuca* for water bioremediation and as feed additive for white shrimp *Litopenaeus vannamei*. **PeerJ** 6: e4459. DOI: 10.7717/peerj.4459.

Food and Agriculture Organization (FAO). 2020. **The State of World Fisheries and Aquaculture 2020–Sustainability in Action.** FAO, Rome, Italy. 224 pp.

Gacia, E., M.M. Littler and D.S. Littler. 1996. The relationships between morphology and photosynthetic parameters within the polymorphic genus *Caulerpa*. **Journal of Experimental Marine Biology and Ecology** 204: 209–224.

Gao, G., A.S. Clare, C. Rose and G.S. Caldwell. 2018. *Ulva rigida* in the future ocean: potential for carbon capture, bioremediation and biomethane production. **GCB Bioenergy** 10: 39–51. DOI: 10.1111/gcbb.12465

Gaylord, B., J.H. Rosman, D.C. Reed, *et al*. 2007. Spatial patterns of flow and their modification within and around a giant kelp forest. **Limnology and Oceanography** 52(5): 1838–1852. DOI: 10.4319/lo.2007.52.5.1838.

Hajisamae, S., P. Madyusoh and H. Mutichun. 2022. **Effect of seaweed on water treatment for mud crab fattening in the recirculating condo system.** Proceedings on Insan Junior Researchers International Conference (IJURECON) 2022: 135–139.

Hurd, C.L. 2000. Water motion, marine macroalgal physiology, and production. **Journal of Phycology** 36(3): 453–472. DOI: 10.1046/j.1529-8817.2000.99139.x.

Jiang, H., D. Zou, W. Lou and Y. Yang. 2017. The photosynthetic responses to stocking depth and algal mat density in the farmed seaweed *Gracilaria lemaneiformis* (Gracilariales, Rhodophyta). **Environmental Science and Pollution Research** 24: 25309–25314. DOI: 10.1007/s11356-017-0198-5.

Johansson, G. and P. Snoeijs. 2002. Macroalgal photosynthetic responses to light in relation to thallus morphology and depth zonation. **Marine Ecology Progress Series** 244: 63–72.

Kang, Y.H., S.R. Park and I.K. Chung. 2011. Biofiltration efficiency and biochemical composition of three seaweed species cultivated in a fish-seaweed integrated culture. **Algae** 26: 97–108. DOI: 10.4490/algae.2011.26.1.097.

Kang, Y.H., S. Kim, S.K. Choi, H.J. Lee, I.K. Chung and S.R. Park. 2021. A comparison of the bioremediation potential of five seaweed species in an integrated fish-seaweed aquaculture system: implication for a multi-species seaweed culture. **Reviews in Aquaculture** 13: 353–364. DOI: 10.1111/raq.12478.

Kunawongdet, P. 2020. Biological water treatment in recirculating aquaculture system by using *Caulerpa lentillifera* J Agardh. **Burapha Science Journal** 25: 509–523. (in Thai)

Lewmanomont, K. and A. Chirapart. 2022. **Biodiversity, cultivation and utilization of seaweeds in Thailand: An overview.** In: Sustainable global resources of seaweeds: Industrial perspectives, Volume 1. (eds. G.A. Ravishankar and A.R. Rao), pp. 91–107. Springer International Publishing, Cham, Switzerland.

Li, G., Z. Qin, J. Zhang, Q. Lin, G. Ni, Y. Tan and D. Zou. 2020. Algal density mediates the photosynthetic responses of a marine macroalga *Ulva conglobata* (Chlorophyta) to temperature and pH changes. **Algal Research** 46: 101797. DOI: 10.1016/j.algal.2020.101797.

Liu, H., F. Wang, Q. Wang, S. Dong and X. Tian. 2016. A comparative study of the nutrient uptake and growth capacities of seaweeds *Caulerpa lentillifera* and *Gracilaria lichenoides*. **Journal of Applied Phycology** 28: 3083–3089. DOI: 10.1007/s10811-016-0858-8.

Manori Bambaranda, B.V.A.S., N. Sasaki, A. Chirapart, K.R. Salin and T.W. Tsusaka. 2019a. Optimization of macroalgal density and salinity for nutrient removal by *Caulerpa lentillifera* from aquaculture effluent. **Process** 7(303): 1–16. DOI: 10.3390/pr7050303.

Manori Bambaranda, B.V.A.S., T.W. Tsusaka, A. Chirapart, K.R. Salin and N. Sasaki. 2019b. Capacity of *Caulerpa lentillifera* in the removal of fish culture effluent in a recirculating aquaculture system. **Process** 7(440): 1–15. DOI: 10.3390/pr7070440.

Mauseth, J.D. 2000. Theoretical aspects of surface-to-volume ratios and water-storage capacities of succulent shoots. **American Journal of Botany** 87(8): 1107–1115. DOI: 10.2307/2656647.

Maxwell, K and G.N. Johnson. 2000. Chlorophyll fluorescence–a practical guide. **Journal of Experimental Botany** 51: 659–668. DOI: 10.1093/jexbot/51.345.659.

Neori, A., T. Chopin, M. Troell, A.H. Buschmann, G.P. Kraemer, C. Halling and C. Yarish. 2004. Integrated aquaculture: rationale, evolution and state of the art emphasizing seaweed biofiltration in modern mariculture. **Aquaculture** 231: 361–391. DOI: 10.1016/j.aquaculture.2003.11.015.

Notification of the Ministry of Natural Resources and Environment. 2004. **The Royal Government Gazette,** Volume 121, Part 49 D. Cabinet and Royal Gazzette Publishing Office, Bangkok, Thailand. 1–4 pp.

Portillo-Clark, G., R. Casillas-Hernández, R. Servín-Villegas and F.J. Magallón-Barajas. 2013. Growth and survival of the juvenile yellowleg shrimp *Farfantepenaeus californiensis* cohabiting with the green feather alga *Caulerpa sertularioides* at different temperatures. **Aquaculture Research** 44: 22–30. DOI: 10.1111/j.1365-2109.2011.03002.x.

Rattanasaensri, S., N. Muangmai, J. Praiboon and A. Chirapart. 2020. Photosynthetic response of filamentous green algae (*Oedogonium*) to irradiance and temperature variations. **Journal of Fisheries and Environment** 44(3): 66–80.

Rees, T.A.V. 2003. Safety factors and nutrient uptake by seaweeds. **Marine Ecology Progress Series** 263: 29–42. DOI: 10.3354/meps263029.

Richards, D.K., C.L. Hurd, D.W. Pritchard, S.R. Wing and C.D. Hepburn. 2011. Photosynthetic response of monospecific macroalgal stands to density. **Aquatic Biology** 13: 41–49. DOI: 10.3354/ab00349.

Rosenberg, G. and J. Ramus. 1984. Uptake of inorganic nitrogen and seaweed surface area: volume ratios **Aquatic Botany** 19: 65–72.

Ruangchuay, R., A. Chirapart and K. Lewmanomont. 2024. **Algae mediated bioremediation in Thailand: An overview.** In: Algae Mediated Bioremediation: Industrial Prospectives, Volume 2. (eds. G.A. Ravishankar, A.R. Rao and S.K. Kim), pp. 683–700. WILEY-VCH GmbH publisher, Weinheim, Germany.

Schreiber, U., H. Hormann, C. Neubauer and C. Klughammer. 1995. Assessment of photosystem II photochemical quantum yield by chlorophyll fluorescence quenching analysis. **Australian Journal of Plant Physiology** 22: 209–220.

Stewart, H.L. and R.C. Carpenter. 2003. The effects of morphology and water flow on photosynthesis of marine macroalgae. **Ecology** 84: 2999–3012. DOI: 10.1890/02-0092.

Suphawinyoo, K., Y. Savangarrom, K. Srisukphu, N. Butwan, S. Rungsang, N. Kannika, C. Somchit and T. Weeplian. 2020. Efficiency of *Gracilaria fisheri* in reducing nitrogen compounds and orthophosphates in water treatment. **Journal of Vocational Institute of Agriculture** 4(1): 39–49. (in Thai)

Taylor, R.B., J.T. A. Peek and T.A.V. Rees. 1998. Scaling of ammonium uptake by seaweeds to surface area:volume ratio: geographical variation and the role of uptake by passive diffusion. **Marine Ecology Progress Series** 169: 143–148.

Thongcanarak, P. and Y. Predalumpaburt. 2008. **Comparison the Efficiency of 4 Seaweed in the Removal of Nitrogen and Phosphate in Effluent from Orange Spotted Grouper (*Epinephelus coioides* Hamilton, 1822) Culture.** Technical Paper No. 40/2008. Coastal Aquaculture Research Institute, Bureau of Coastal Fisheries Research and Development, Department of Fisheries, Ministry of Agriculture and Cooperatives. Bangkok, Thailand. 32 pp. (in Thai)

Vogel, S. 1988. **Life's Devices: The Physical World of Animals and Plants.** Princeton University Press, Princeton, New Jersey, USA. 384 pp.